Hindawi Publishing Corporation
Journal of Nanomaterials
Volume 2015, Article ID 502514, 7 pages
http://dx.doi.org/10.1155/2015/502514

Research Article

Facile Preparation of Efficient WO_3 Photocatalysts Based on Surface Modification

Min Liu,[1,2] Hongmei Li,[1] and Yangsu Zeng[1]

[1]*Institute of Laser and Information, Department of Information Engineering, Shaoyang University, Hunan 42200, China*
[2]*School of Engineering, The University of Tokyo, 7-3-1 Hongo, Bunkyo-ku, Tokyo 113-8656, Japan*

Correspondence should be addressed to Hongmei Li; hongmeili82@gmail.com and Yangsu Zeng; yangsuz@vip.sina.com

Received 8 February 2015; Revised 4 August 2015; Accepted 17 August 2015

Academic Editor: Sherine Obare

Tungsten trioxide (WO_3) was surface modified with Cu(II) nanoclusters and titanium dioxide (TiO_2) nanopowders by using a simple impregnation method followed by a physical combining method. The obtained nanocomposites were studied by scanning electron microscope, X-ray photoelectron spectroscopy spectra, UV-visible light spectra, and photoluminescence, respectively. Although the photocatalytic activity of WO_3 was negligible under visible light irradiation, the visible light photocatalytic activity of WO_3 was drastically enhanced by surface modification of Cu(II) nanoclusters and TiO_2 nanopowders. The enhanced photocatalytic activity is due to the efficient charge separation by TiO_2 and Cu(II) nanoclusters functioning as cocatalysts on the surface. Thus, this simple strategy provides a facile route to prepare efficient visible-light-active photocatalysts for practical application.

1. Introduction

As one of the most important transition metal oxides, tungsten trioxide (WO_3) has attracted considerable attention due to its promising physical and chemical properties [1, 2]. Considering its small band gap, stable physicochemical properties and resilience to photocorrosion effects, WO_3 has been widely considered as a feasible candidate for visible-light photocatalysts [1–3]. However, several fundamental issues have to be addressed before they are economically available for large scale industrial applications. For example, pure WO_3 is usually not efficient photocatalysts because of the high electron-hole recombination rate and the difficulty in the reduction of oxygen, due to the negative position of its conduction band (CB) [4]. Thus, many efforts have been made to improve the activity of WO_3, such as morphology control, doping, nanostructure construction, and surface modification [4]. One of the most promising ways to accomplish this goal is to design heterogeneous catalysts [5]. So far, various heterogeneous WO_3 based heterogeneous structures, such as WO_3/SiO_2, WO_3/TiO_2, WO_3/NiO, and Pt/TiO_2-WO_3, have been designed toward good catalytic performance [5–12].

Titanium dioxide (TiO_2) has attracted much attention as a suitable semiconductor to construct heterogeneous structures with WO_3, due to its low cost, nontoxicity, and suitable band structure [5, 13–16]. The valence band (VB) and CB potentials of TiO_2 are more cathodic than those of WO_3 [16]. The coupling of TiO_2 and WO_3 can lead to photogenerated electron and hole transfer from one semiconductor particle to another; those are electrons transfer from the CB of TiO_2 down to the CB of WO_3 and holes transfer from the VB of WO_3 to that of TiO_2 [17]. This process suppresses the recombination of photogenerated carriers and leads to improved photocatalytic efficiency of the system [17]. To further increase the photocatalytic performance of the system, metal or metal oxide particles, such as Au, Pt, and CuO, were introduced into the system to promote the reduction reaction of electrons with oxygen molecules, leading to efficient consumption of electrons [10–12]. For example, copper ions modified WO_3/TiO_2 nanocomposites, prepared by Hosogi and Kuroda, exhibited efficient photocatalytic activities [12]. However, there are still many problems in the practical application of these reported catalysts, including the complexity of the preparation procedures, the requirement

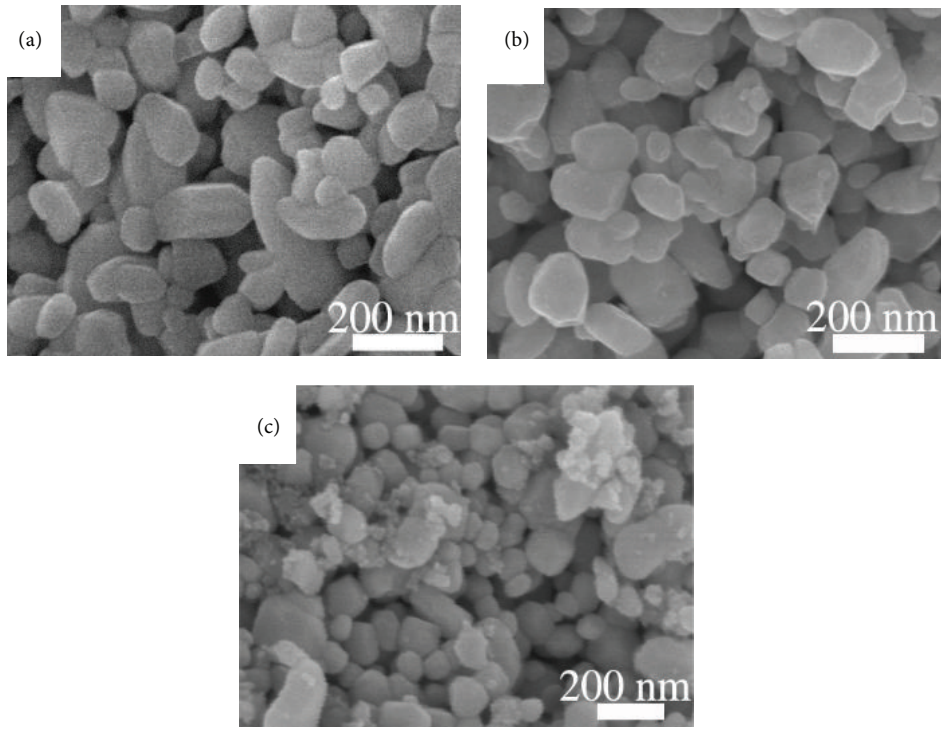

Figure 1: SEM images of bare WO_3 (a), Cu(II)-WO_3 (b), and Cu(II)-WO_3/TiO_2 (c).

for expensive raw materials, and the difficulties for large scale production [5–12]. For instance, sol-gel method and urea as raw materials were needed in the preparation of copper ions modified WO_3/TiO_2 nanocomposites [12]. Thus, efforts aimed at improving the photocatalytic performance and the preparation process of WO_3 are still needed.

In the present work, we reported efficient Cu(II) nanoclusters modified WO_3/TiO_2 nanocomposites (Cu(II)-WO_3/TiO_2) through a facile preparation process. In this process, Cu(II) nanoclusters were deposited on WO_3 using a simple impregnation method and TiO_2 nanopowders were introduced into the Cu(II) nanoclusters modified WO_3 (Cu(II)-WO_3) by a physical combination method. The introduced Cu(II) nanoclusters and TiO_2 nanopowders functioned as cocatalysts on the surface of WO_3. Thus, the obtained Cu(II)-WO_3/TiO_2 products exhibited an enhanced visible light photocatalytic activity.

2. Experimental

2.1. Materials. Commercial tungsten (VI) oxide (Sigma-Aldrich; for monoclinic WO_3, particle size is ~100 nm) was used as the initial WO_3. $CuCl_2{\cdot}2H_2O$ (Sigma-Aldrich) was used as the source of Cu(II) nanoclusters. Degussa (Evonik) P25 TiO_2 nanopowders (particle size ~25 nm) was used as the raw material of TiO_2. All of these commercial materials were used as received, without further purification. Distilled water was applied in the experimental process.

2.2. Preparation of the Composites. Cu(II) nanoclusters were grafted on the surface of WO_3 by using an impregnation method, as reported previously [18, 19]. $CuCl_2{\cdot}2H_2O$ was used as the Cu(II) nanoclusters source to prepare Cu(II)-WO_3. 1 g WO_3 powder with 0.1% weight fraction of Cu to WO_3 was dispersed in 10 mL distilled water. 0.1% weight fraction of Cu to WO_3 has demonstrated the optimized amount of Cu(II) nanoclusters for Cu(II)-WO_3 systems [18]. The suspension was heated at 90°C and stirred for 1 h in a vial reactor to hydrolyze the $CuCl_2$ source and generate Cu(II) nanoclusters on the surface of WO_3. Then, the suspension was filtered twice with a membrane filter (0.025 μm, Millipore) and washed with sufficient amounts of distilled water. The resulting residue was dried at 110°C for 24 h and subsequently grounded into fine powder using an agate mortar and pestle.

The mixing of Cu(II)-WO_3 with TiO_2 was performed using a physical mixing method. Typically, 1 g Cu(II)-WO_3 powder and 1% weight ratio TiO_2 were mixed in an agate mortar and grounded into fine powder using a pestle for 1 h.

2.3. Sample Characterizations. Scanning electron microscope (SEM) images were taken using a field-emission SEM (FE-SEM, Hitachi S-4800). Photoluminescence PL spectra were obtained by using a Hitachi F-4500 fluorophotometer with an excited wavelength of λ = 325 nm at room temperature. UV-visible reflectance spectra were obtained by the diffuse reflection method using a spectrometer (UV-2550, Shimadzu). Surface compositions were studied by X-ray photoelectron spectroscopy (XPS; model 5600, Perkin-Elmer). The binding energy data were calibrated with reference to the C 1s signal at 284.5 eV.

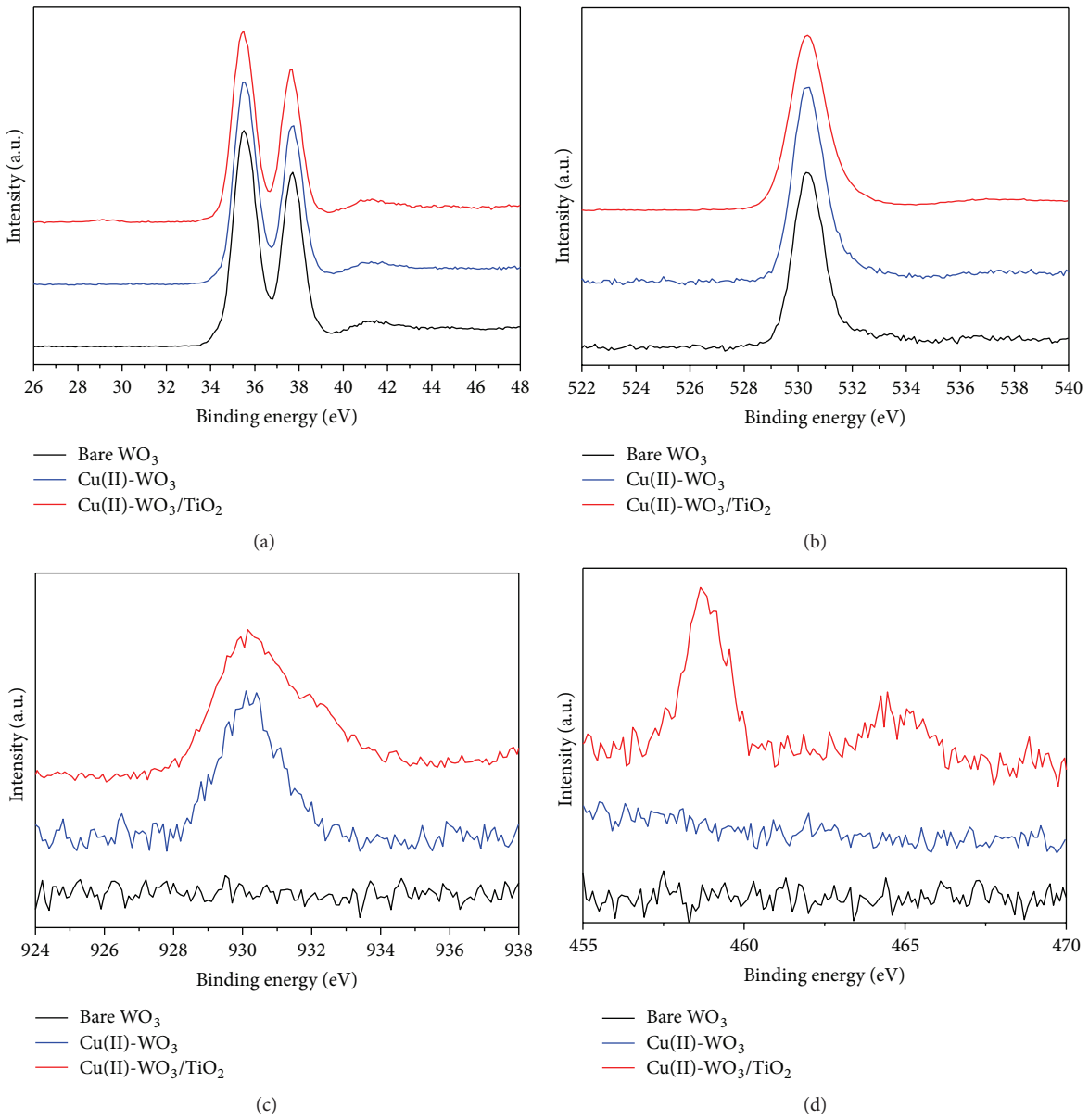

Figure 2: (a) W 4f core-level spectra, (b) O 1s core-level spectra, (c) Cu 2p core-level spectra, and (d) Ti 2p core-level spectra of bare WO_3, Cu(II)-WO_3, and Cu(II)-WO_3/TiO_2, respectively.

2.4. Catalytic Activity Testing. Photocatalytic activity of the WO_3 samples was evaluated in terms of the decolorization of methylene blue (MB) dye under visible irradiation. 20 mg sample was dispersed into 100 mL of 10 mg/L MB solution and stirred in the dark for 1 h to reach a complete adsorption-desorption equilibrium. Then the solution was irradiated with ~20 mW/cm^2 visible light (>420 nm, with a light filter L42 (Asahi Techno-Glass)) under continuous stirring. With a given irradiation time interval, some specimens (5 mL) were taken from the dispersion and were centrifuged (4000 rpm). The clear upper solution was subjected to UV-Vis spectrophotometer (UV-2550, Shimadzu). The concentration of MB was determined from the absorbance at the wavelength of 665 nm.

3. Results

Figure 1 shows the SEM images of the obtained samples. It can be seen that the bare WO_3 samples contained many particles. These particles have a clear surface and a size of ~100 nm. After Cu(II) nanoclusters grafting, the particle morphology still remained, indicating the grafting of Cu(II) nanoclusters did not affect its morphology (Figure 1(b)). After the modification with TiO_2 nanopowders, some small particles could be observed in TiO_2 mixed Cu(II)-WO_3 (Cu(II)-WO_3/TiO_2) samples (Figure 1(c)). These small particles have a size around several tens of nanometers, coinciding with the size of TiO_2 nanopowders. In the paper, except specially noted, the weight ratios of Cu and TiO_2 to WO_3 were set to 0.1% and 1%, respectively,

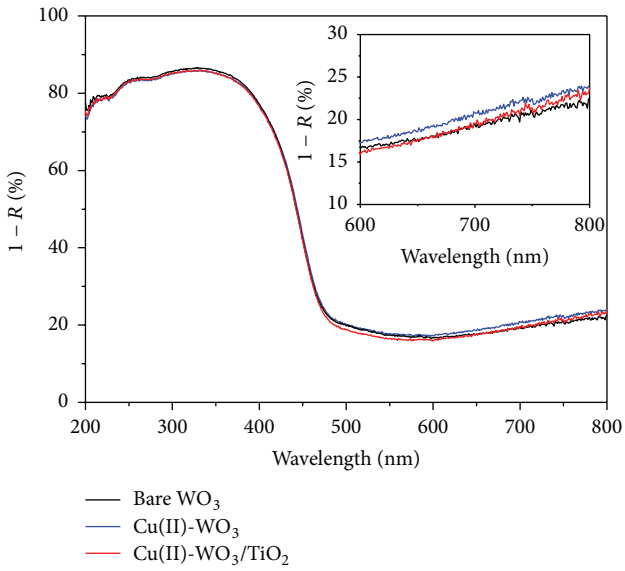

FIGURE 3: UV-visible reflectance spectra of bare WO_3, Cu(II)-WO_3, and Cu(II)-WO_3/TiO_2, respectively. Inset is the enlarged UV-visible reflectance spectra at range of 600–800 nm.

In order to determine the surface composition and chemical states of the surface elements, XPS spectra were recorded, as shown in Figure 2. In the W 4f and O 1s core-level spectra of the samples (Figures 2(a) and 2(b)), no obvious differences could be seen in the chemical states of elements W and O, demonstrating that neither the surface grafting of Cu(II) nanoclusters nor physical mixing of TiO_2 powders affected the bonding structure between tungsten and oxygen. In the Cu 2p core-level spectra (Figure 2(c)), Cu signals were clearly observed in Cu(II)-grafted samples, such as Cu(II)-WO_3 and Cu(II)-WO_3/TiO_2, confirming that Cu(II) was successfully grafted on the surface of WO_3, while, in the Ti 2p core-level spectra (Figure 2(d)), Ti signal was only observed in Cu(II)-WO_3/TiO_2 composites, indicating the TiO_2 was well mixed with WO_3 powders.

Figure 3 shows the UV-Vis of the samples. It clearly shows that WO_3 has a good visible light absorption property, indicating it is a potential visible light photocatalyst. The absorption edge of WO_3 is located at ~460 nm, which corresponds to the interband transition of WO_3 [18]. This interband absorption indicates a band gap of ~2.7 eV, which coincides with the reported values of 2.7 eV for WO_3 [20, 21]. After Cu(II) nanoclusters grafting, an additional light absorption at the range of ~700–800 nm was clearly superimposed on the light absorption of WO_3, as shown in the inset of Figure 3. This additional light absorption can be attributed to the d-d transition of Cu(II) [18]. After further modification with TiO_2 powders, the interband transition of WO_3 was not changed, due to the small amount of TiO_2 powders and their large band gap [13–15]. Notably, the additional visible light absorption caused by the d-d transition of Cu(II) can still be observed in the mixed nanocomposites, proving the existence of Cu(II) nanoclusters (inset of Figure 3).

Figure 4 represents the variation of MB concentration by photocatalytic reaction with the samples under visible light (>420 nm) irradiation. Typical evolution of MB concentration during photocatalytic reaction on Cu(II)-WO_3/TiO_2 is presented in Figure 4(a). Under light irradiation, the characteristic MB absorption peak decreased sharply and almost no color was observed after 90 minutes of irradiation, indicating that MB was completely degraded by Cu(II)-WO_3/TiO_2. Comparative studies among bare WO_3, Cu(II)-WO_3, and Cu(II)-WO_3/TiO_2 show that bare WO_3 has a negligible activity under visible light irradiation (Figure 4(b)). The grafting of Cu(II) nanoclusters to the surface switched its photocatalytic activity. It can be seen that MB dye was almost degraded by Cu(II)-WO_3 with 2 h of visible light irradiation. Interestingly, after further modification with TiO_2 nanopowders, Cu(II)-WO_3/TiO_2 exhibited an enhanced photocatalytic activity compared with that of Cu(II)-WO_3. MB dye was completely degraded by Cu(II)-WO_3/TiO_2 nanocomposites with 1.5 h of visible light irradiation, revealing the high photocatalytic activity of the Cu(II)-WO_3/TiO_2 nanocomposites. Figure 4(c) shows the pseudo-first-order kinetic rate for the photochemical degradation of MB by Cu(II)-TiO_2 samples. The pseudo-first-order kinetic rate was calculated according to the equation of $\ln(C_o/C) = kt$, where C/C_o is the normalized MB concentration, t is the reaction time, and k is the pseudo-first-rate constant. It can been seen that the Cu(II)-WO_3/TiO_2 samples presented the highest reaction rate. The reaction rate was sharply decreased when bare WO_3 was used. The result was consistent with the MB decomposition curves in Figure 4(b). Figure 4(d) shows the cycling measurements of MB decomposition over Cu(II)-WO_3/TiO_2. Similar k values were obtained after 5-cycle measurements, suggesting a good stability for the photocatalytic application of Cu(II)-WO_3/TiO_2.

We also investigated the influences of experimental parameters on the photocatalytic performances of Cu(II)-WO_3/TiO_2 samples. Figure 5 shows the photocatalytic performances of Cu(II)-WO_3/TiO_2 samples with different ratios of TiO_2. It can be seen that the activity of the samples was increased with the ratio of TiO_2 to WO_3 in the beginning. After the highest activity was achieved at the ratio of 1%, the photocatalytic activity was decreased again with the increase of ratio. These results revealed that the Cu(II)-WO_3/TiO_2 samples obtained with 1% TiO_2 have the optimum amount of TiO_2 for hole separation and reaction. It has been reported that the amount of TiO_2 to mix with WO_3 was important for the photocatalytic reaction [22, 23]. Thus, the Cu(II)-WO_3/TiO_2 samples with a TiO_2 ratio of 1% exhibited the highest photocatalytic performance.

4. Discussions

Figure 6 shows the energy levels of TiO_2 and WO_3 [18]. TiO_2, as one of the most efficient photocatalysts, has a high potential CB and a deep VB. Thus, electrons in its CB have sufficient reduction power for oxygen reaction with single electron and holes in its VB have large oxidation power for organic compounds decomposition, respectively. Consequently, TiO_2 has a very high efficiency for photocatalytic reactions under

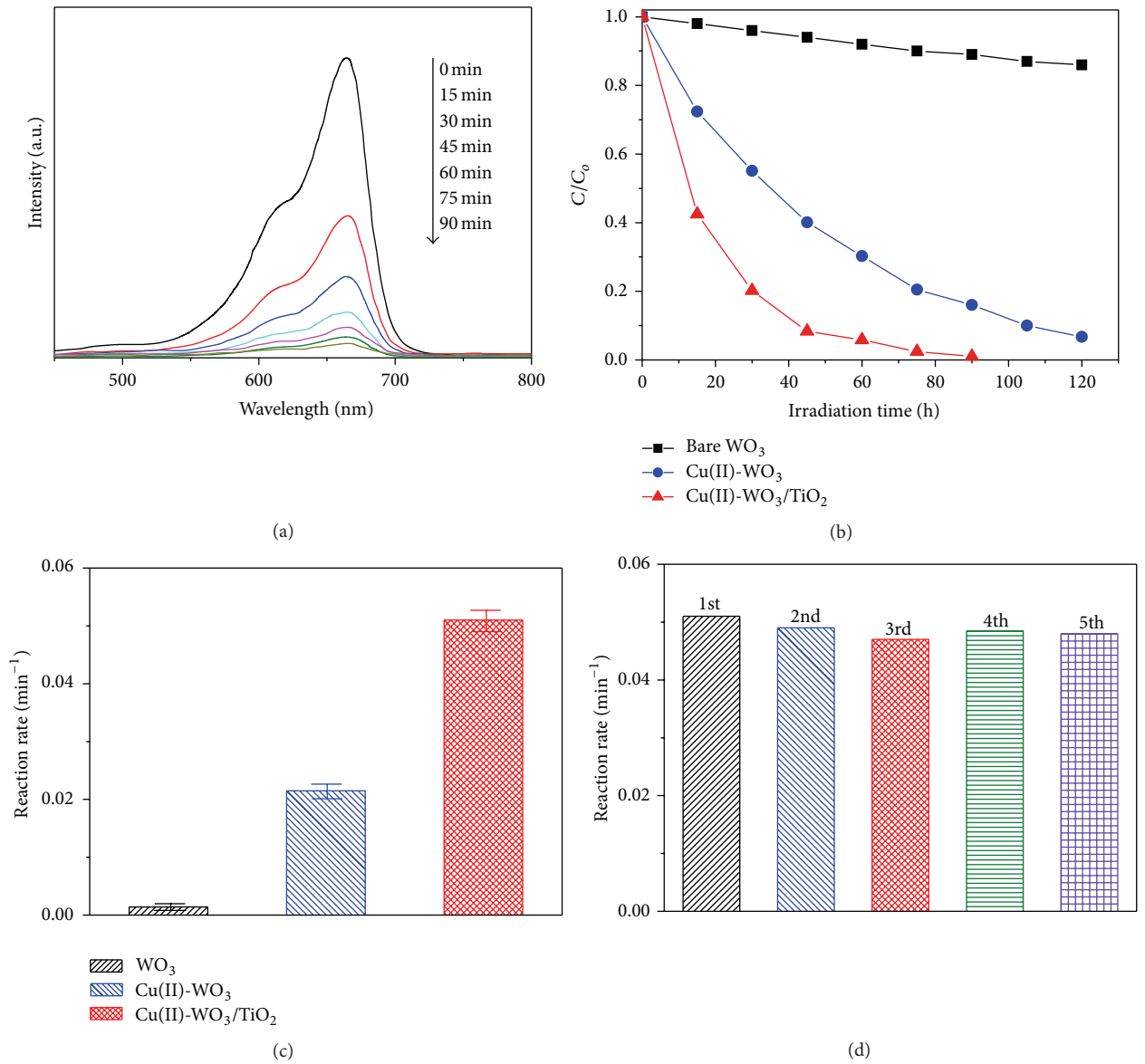

Figure 4: (a) Absorption spectra for MB degradation using Cu(II)-WO_3/TiO_2. (b) The variation of MB concentration by photocatalytic reaction with bare WO_3, Cu(II)-WO_3, and Cu(II)-WO_3/TiO_2, respectively. (c) The pseudo-first-order kinetic rates with error bars for the photochemical degradation of MB by bare WO_3, Cu(II)-WO_3, and Cu(II)-WO_3/TiO_2, respectively. (d) Cycling measurements of MB decomposition over Cu(II)-WO_3/TiO_2.

UV light irradiation. However, TiO_2 can only be activated under UV light irradiation, owing to its large band gap. WO_3 is sensitive to visible light because of its proper band gap, 2.7 eV [20, 21]. Notably, both the CB and VB positions of WO_3 are more positive than those of TiO_2. As a result, photogenerated electrons can be transferred from the CB of TiO_2 to the CB of WO_3 and photogenerated holes can be transferred from the VB of WO_3 to that of TiO_2 [17]. Moreover, if photons do not have enough energy to excite TiO_2 but have enough energy to excite WO_3, hole in the VB of WO_3 is still possibly transferred to the VB of TiO_2 [24]. This process suppresses the recombination of photogenerated carriers and indicates that TiO_2 can act as hole cocatalyst [12, 17, 24]. On the other hand, the CB potential of WO_3 is lower than the potential for reduction reaction of oxygen molecules, leading to the insufficient consumption of electrons in CB. When Cu(II) nanoclusters were modified on the surface of WO_3, the photogenerated electrons in the CB of WO_3 can be transferred to the Cu(II) nanoclusters. The transferred electrons can be consumed by multielectron reduction reactions with oxygen molecules in the Cu(II) nanoclusters [18, 19]. In other words, Cu(II) nanoclusters function as efficient electron cocatalysts [12, 18, 19]. Consequently, the activity of Cu(II)-WO_3 can be further enhanced by combining with TiO_2.

Figure 7 shows the PL spectra of bare WO_3, Cu(II)-WO_3, and Cu(II)-WO_3/TiO_2, respectively. The main emission peak for WO_3 is centered at about 460 nm, which is approximately equal to the band gap energy of WO_3 [20, 25]. It worth noting

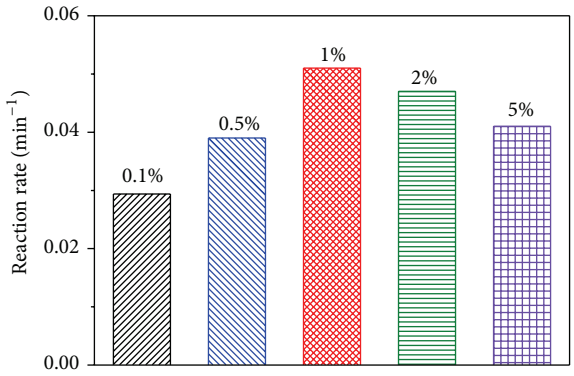

Figure 5: Photocatalytic activities of Cu(II)-WO_3/TiO_2 samples with different ratios of TiO_2.

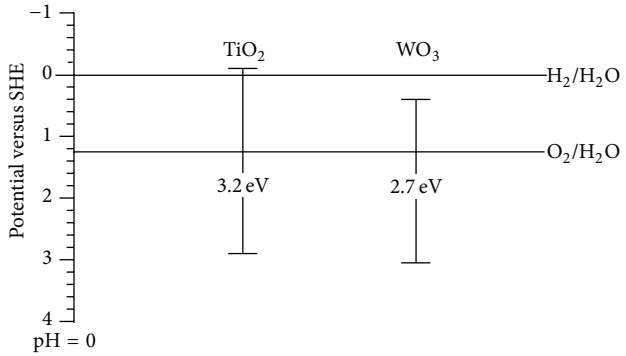

Figure 6: Energy levels of TiO_2 and WO_3.

that bare WO_3 exhibited the highest PL intensity among these samples, indicating the highest recombination rate of electrons and holes [26]. After the Cu(II) nanoclusters were grafted, the intensity of the PL emission decreases, which can be attributed to the decrease of the efficient electron trapping and consumption on Cu(II) nanoclusters [18, 19]. The emission intensity of the Cu(II)-WO_3/TiO_2 was lower than that of bare WO_3 and Cu(II)-WO_3, which indicated that the recombination rate of photogenerated charge carriers was the lowest in the Cu(II)-WO_3/TiO_2. The PL results confirmed the importance of the modification of Cu(II) nanoclusters and TiO_2 nanopowders for hindering the recombination of electrons and holes. Thus, efficient visible light photocatalytic activity can be achieved in Cu(II) and TiO_2 modified WO_3.

5. Conclusions

Efficient WO_3 photocatalysts were prepared by being simply surface modified with Cu(II) nanoclusters and TiO_2 nanopowders. In this prepared system, Cu(II) nanoclusters and TiO_2 nanopowders were deposited on the surface of WO_3 using a simple impregnation method and a physical combination method, respectively. Cu(II) nanoclusters and TiO_2 nanopowders functioned as efficient cocatalysts on the surface of WO_3, which acted as photocatalyst. Thus, efficient charge separations and reactions can be achieved in this Cu(II)-WO_3/TiO_2 system, resulting in efficient visible light photocatalytic reaction for organic compounds decomposition. The simple strategy opens an avenue for designing efficient visible-light-active photocatalysts for practical application.

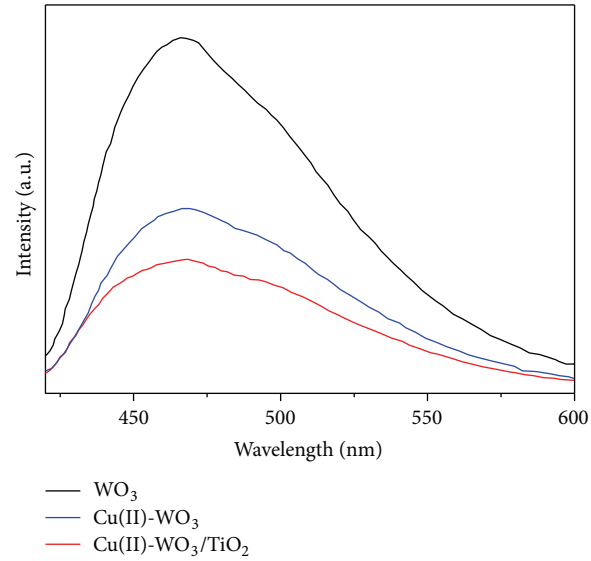

Figure 7: PL spectra of bare WO_3, Cu(II)-WO_3, and Cu(II)-WO_3/TiO_2, respectively.

Conflict of Interests

The authors declare that there is no conflict of interests regarding the publication of this paper.

Acknowledgments

This work was supported by the Scientific Research Fund of Hunan Provincial Education Department under Grant no. 09A083 and the Science and Technology Fund of Hunan Provincial Science and Technology Department under Grant no. 2012FJ4137.

References

[1] J. Zhou, Y. Ding, S. Z. Deng, L. Gong, N. S. Xu, and Z. L. Wang, "Three-dimensional tungsten oxide nanowire networks," *Advanced Materials*, vol. 17, no. 17, pp. 2107–2110, 2005.

[2] G. C. Xi, Y. Yan, Q. Ma et al., "Synthesis of multiple-shell WO_3 hollow spheres by a binary carbonaceous template route and their applications in visible-light photocatalysis," *Chemistry*, vol. 18, no. 44, pp. 13949–13953, 2012.

[3] D. L. Chen, L. Gao, A. Yasumori, K. Kuroda, and Y. Sugahara, "Size- and shape-controlled conversion of tungstate-based inorganic-organic hybrid belts to WO_3 nanoplates with high specific surface areas," *Small*, vol. 4, no. 10, pp. 1813–1822, 2008.

[4] X. An, J. C. Yu, Y. Wang, Y. Hu, X. Yu, and G. Zhang, "WO_3 nanorods/graphene nanocomposites for high-efficiency visible-light-driven photocatalysis and NO_2 gas sensing," *Journal of Materials Chemistry*, vol. 22, no. 17, pp. 8525–8531, 2012.

[5] X.-L. Yang, W.-L. Dai, C. W. Guo et al., "Synthesis of novel core-shell structured WO_3/TiO_2 spheroids and its application

in the catalytic oxidation of cyclopentene to glutaraldehyde by aqueous H_2O_2," *Journal of Catalysis*, vol. 234, no. 2, pp. 438–450, 2005.

[6] A. Spamer, T. I. Dube, D. J. Moodley, C. van Schalkwyk, and J. M. Botha, "Application of a WO_3/SiO_2 catalyst in an industrial environment: part II," *Applied Catalysis A: General*, vol. 255, no. 2, pp. 133–142, 2003.

[7] R. H. Jin, X. Xia, W. L. Dai, J. F. Deng, and H. X. Li, "An effective heterogeneous WO_3/TiO_2–SiO_2 catalyst for selective oxidation of cyclopentene to glutaraldehyde by H_2O_2," *Catalysis Letters*, vol. 62, no. 2–4, pp. 201–207, 1999.

[8] M. Bao, Y. J. Chen, F. Li et al., "Plate-like p-n heterogeneous NiO/WO_3 nanocomposites for high performance room temperature NO_2 sensors," *Nanoscale*, vol. 6, no. 8, pp. 4063–4066, 2014.

[9] A. K. Nayak, R. Ghosh, S. Santra, P. K. Guha, and D. Pradhan, "Hierarchical nanostructured WO_3–SnO_2 for selective sensing of volatile organic compounds," *Nanoscale*, vol. 7, no. 29, pp. 12460–12473, 2015.

[10] M.-H. Chen, C.-S. Lu, and R.-J. Wu, "Novel Pt/TiO_2-WO_3 materials irradiated by visible light used in a photoreductive ozone sensor," *Journal of the Taiwan Institute of Chemical Engineers*, vol. 45, no. 3, pp. 1043–1048, 2014.

[11] R.-J. Wu, Y.-C. Chiu, C.-H. Wu, and Y.-J. Su, "Application of Au/TiO_2–WO_3 material in visible light photoreductive ozone sensors," *Thin Solid Films*, vol. 574, pp. 156–161, 2015.

[12] Y. Hosogi and Y. Kuroda, "Tungsten oxide photocatalyst and method for producing the same," US Patent, US 8652991 B2, 2014.

[13] T. L. Thompson and J. T. Yates Jr., "Surface science studies of the photoactivation of TiO_2—new photochemical processes," *Chemical Reviews*, vol. 106, no. 10, pp. 4428–4453, 2006.

[14] X. Chen and S. S. Mao, "Titanium dioxide nanomaterials: synthesis, properties, modifications and applications," *Chemical Reviews*, vol. 107, no. 7, pp. 2891–2959, 2007.

[15] H. Li, Y. Zeng, T. Huang, L. Piao, and M. Liu, "Controlled synthesis of anatase TiO_2 single crystals with dominant {001} facets from TiO $_2$ powders," *ChemPlusChem*, vol. 77, no. 11, pp. 1017–1021, 2012.

[16] M. Liu, H. Li, Y. Zeng, and T. Huang, "Anatase TiO_2 single crystals with dominant {001} facets: facile fabrication from Ti powders and enhanced photocatalytical activity," *Applied Surface Science*, vol. 274, pp. 117–123, 2013.

[17] M. M. Khan, M. O. Ansari, D. H. Han, and M. H. Cho, "Band gap engineered TiO_2 nanoparticles for visible light induced photoelectrochemical and photocatalytic studies," *Journal of Materials Chemistry A*, vol. 2, pp. 637–644, 2014.

[18] H. Irie, S. Miura, K. Kamiya, and K. Hashimoto, "Efficient visible light-sensitive photocatalysts: grafting Cu(II) ions onto TiO_2 and WO_3 photocatalysts," *Chemical Physics Letters*, vol. 457, pp. 202–204, 2008.

[19] H. Irie, K. Kamiya, T. Shibanuma et al., "Visible light-sensitive Cu(II)-grafted TiO_2 photocatalysts: activities and X-ray absorption fine structure analyses," *Journal of Physical Chemistry C*, vol. 113, no. 24, pp. 10761–10766, 2009.

[20] G. R. Bamwenda, K. Sayama, and H. Arakawa, "The effect of selected reaction parameters on the photoproduction of oxygen and hydrogen from a WO_3-Fe^{2+}-Fe^{3+} aqueous suspension," *Journal of Photochemistry and Photobiology A: Chemistry*, vol. 122, no. 3, pp. 175–183, 1999.

[21] T. Arai, M. Yanagida, Y. Konishi, Y. Iwasaki, H. Sugihara, and K. Sayama, "Efficient complete oxidation of acetaldehyde into CO_2 over $CuBi_2O_4/WO_3$ composite photocatalyst under visible and UV light irradiation," *The Journal of Physical Chemistry C*, vol. 111, no. 21, pp. 7574–7577, 2007.

[22] W. Smith, A. Wolcott, R. C. Fitzmorris, J. Z. Zhang, and Y. Zhao, "Quasi-core-shell TiO_2/WO_3 and WO_3/TiO_2 nanorod arrays fabricated by glancing angle deposition for solar water splitting," *Journal of Materials Chemistry*, vol. 21, no. 29, pp. 10792–10800, 2011.

[23] J. Papp, S. Soled, K. Dwight, and A. Wold, "Surface acidity and photocatalytic activity of TiO_2, WO_3/TiO_2, and MoO_3/TiO_2 photocatalysts," *Chemistry of Materials*, vol. 6, no. 4, pp. 496–500, 1994.

[24] S. Y. Chai, Y. J. Kim, and W. I. Lee, "Photocatalytic WO_3/TiO_2 nanoparticles working under visible light," *Journal of Electroceramics*, vol. 17, no. 2–4, pp. 909–912, 2006.

[25] T. Arai, M. Yanagida, Y. Konishi, Y. Iwasaki, H. Sugihara, and K. Sayama, "Efficient complete oxidation of acetaldehyde into CO_2 over $CuBi_2O_4/WO_3$ composite photocatalyst under visible and UV light irradiation," *Journal of Physical Chemistry C*, vol. 111, no. 21, pp. 7574–7577, 2007.

[26] L. L. Chen, W. X. Zhang, C. Feng, Z. H. Yang, and Y. M. Yang, "Replacement/etching route to ZnSe nanotube arrays and their enhanced photocatalytic activities," *Industrial and Engineering Chemistry Research*, vol. 51, no. 11, pp. 4208–4214, 2012.